

1352-2310(95)00130-1

IMPACT OF TORONTO URBAN EMISSIONS ON OZONE LEVELS DOWNWIND

XIUDE LIN, PASCAL B. ROUSSEL, STEVEN LASZLO, RON TAYLOR
and OCTAVIO T. MELO

Ontario Hydro Technologies, 800 Kipling Avenue, Toronto, Ont., Canada M8Z 5S4

and

PAUL B. SHEPSON, DON R. HASTIE and HIROMI NIKI

Department of Chemistry/Centre for Atmospheric Chemistry, York University, 4700 Keele St.,
North York, Ont., Canada M3J 1P3

Abstract—During the 1992 Southern Ontario Oxidants Study (SONTOS 92), an impingement of the Greater Toronto urban plume was observed in the late afternoon of 6 August at the Hastings monitoring site, 140 km to the northeast of the Toronto urban core. Associated with the start of the impingement, sharp increases in the concentration of O₃ and other species were observed. A 1D photochemical transport model was used to investigate this event further.

The 1D model was first exercised in an Eulerian mode to generate two initial chemical systems, one for the air parcel associated with the Greater Toronto urban core and the other characterizing the background. Lagrangian calculations with the 1D model were then conducted following both the urban plume and the background air parcels. When consecutive plume puffs passed over preset virtual receptors, the time of passage and species concentrations, both within the plume and in the background air, were registered. The calculated and measured changes in the concentrations of O₃, PAN, NO_x and hydrocarbon compounds due to the urban plume impingement are in reasonable agreement. Further sensitivity studies were conducted and the factors affecting the impact of the Greater Toronto urban plume are discussed.

Key word index: Urban emission, ozone, NO_x, VOC.

1. INTRODUCTION

Urban areas, as important anthropogenic sources of O₃ precursors, exert significant impacts on local and regional O₃ levels. Previous work has been carried out for various urban areas in North America (e.g. White and Patterson, 1983; Angle and Sandhu, 1989; Leahey and Hansen, 1990; Gladstone *et al.*, 1991; Sillman *et al.*, 1993). During the 1992 Southern Ontario Oxidants Study (SONTOS 92), two extensive ground-level monitoring sites were set up and operated in southern Ontario (Roussel *et al.*, 1994). One of the objectives of SONTOS 92 was to study the effect of the Greater Toronto urban emissions on O₃ level downwind. The two monitoring sites of SONTOS 92 were located in Hastings and Binbrook. The Hastings site is about 140 km to the NE of Toronto while the Binbrook site is about 80 km to the SW of Toronto (see Fig. 1). Ozone, nitrogen species, CO, SO₂, VOCs and meteorological parameters were

measured at both the sites. Since SW winds predominate during the Summer in this region, this SW-NE alignment enhances the chances of catching the Greater Toronto urban plume, enabling us to study the effect of the Toronto urban emissions downwind.

On 6 August 1992, southern Ontario was within a clear air mass moving from the NW. During the day, the wind direction as measured at both Binbrook and Hastings sites varied slowly between westerly and southerly. The average wind speed was about 2.5 m s⁻¹. The measured daily maximum temperature (in the afternoon) in the region was around 25°C. In the late afternoon, the concentrations of several key species at the Hastings site increased abruptly and simultaneously around 17:30 EDT (eastern daylight time, one hour ahead of eastern standard time). As shown in Figs 2 and 3, NO and NO₂ surged from 0.2 and 1 ppb to 0.4 and 4 ppb, respectively; and CO, a good tracer for urban air emissions, jumped from 200 to 450 ppb.

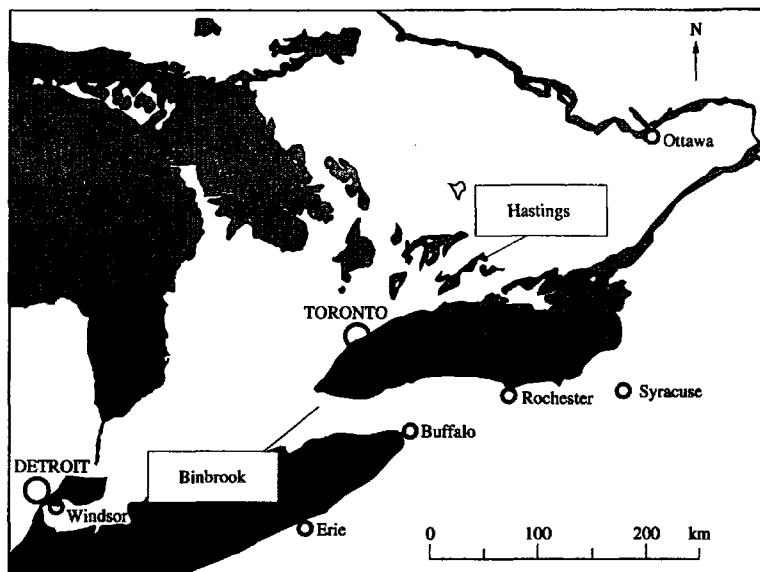


Fig. 1.

It is noted that Figs 2 and 3 also show morning peaks for these species. These morning peaks were caused by emissions from the local rush-hour traffic before the break-up of the nocturnal inversion layer in the morning. In the afternoon, however, measured temperature gradient between 1 and 9 m above ground indicated that the onset of the nocturnal inversions did not occur until 19:00 EDT at the Hastings site (Roussel *et al.*, 1994). Thus, local emissions from the afternoon rush hours were well mixed in the PBL and could not induce a second maximum for the primary pollutants before 19:00 EDT. This is corroborated by the averaged diurnal variations of NO observed at the Hastings site (Roussel *et al.*, 1994). The abrupt increases of NO, NO₂ and CO levels may be associated with the impingement of the Greater Toronto urban plume.

The above assumption is further supported by the measurements of two photochemical products, O₃ and PAN, at Hastings. As shown in Figs 4 and 5, O₃ jumped from 43 to 68 ppb while PAN rose from 0.3 to 1.2 ppb at 17:30 EDT on 6 August 1992. The abrupt increases in concentration of these secondary pollutants indicate a shift between two different air parcels at this time rather than fluctuations due to local emissions. In addition, measurements of VOCs (canister grab samples) also showed some abnormal variations. Figure 6 presents the measured levels of several key VOCs from nine samples taken at the Hastings site on 6 August. It is evident that the levels of C₃H₈, C₄H₁₀, C₂H₄ and toluene increased by a factor of more than four from the sampling

immediately before 17:30 EDT to the next one after. Synthesizing the above evidences, it can be reasonably assumed that the Greater Toronto urban plume impinged on the Hastings site around 17:30 EDT on 6 August 1992.

This event of the Toronto plume impingement gives us a good opportunity to study the impact of the Greater Toronto urban emissions on O₃ levels downwind. In this preliminary study, we use a 1D photochemical transport model to simulate the variations of various chemical species associated with the impingement event. In the following section, a brief description of the model used in the study is provided. The preparation of initial conditions used for the various model runs is presented in Section 3. Model simulations and discussion are given in Section 4 while Section 5 provides concluding remarks.

2. BRIEF DESCRIPTION OF THE MODEL

The 1D photochemical transport model used in the study is composed of an explicit photochemical mechanism and a vertical transport module. These two components have been used in various studies (Liu *et al.*, 1987, 1988, 1992; Trainer *et al.*, 1987, 1991). Briefly, the photochemistry module consists of 146 gas-phase reactions involving 76 species. The mechanism includes the most important reactions of alkanes, alkenes and aromatics, related to O₃ photochemistry in the troposphere, and includes both anthropogenic and natural hydrocarbons. In the

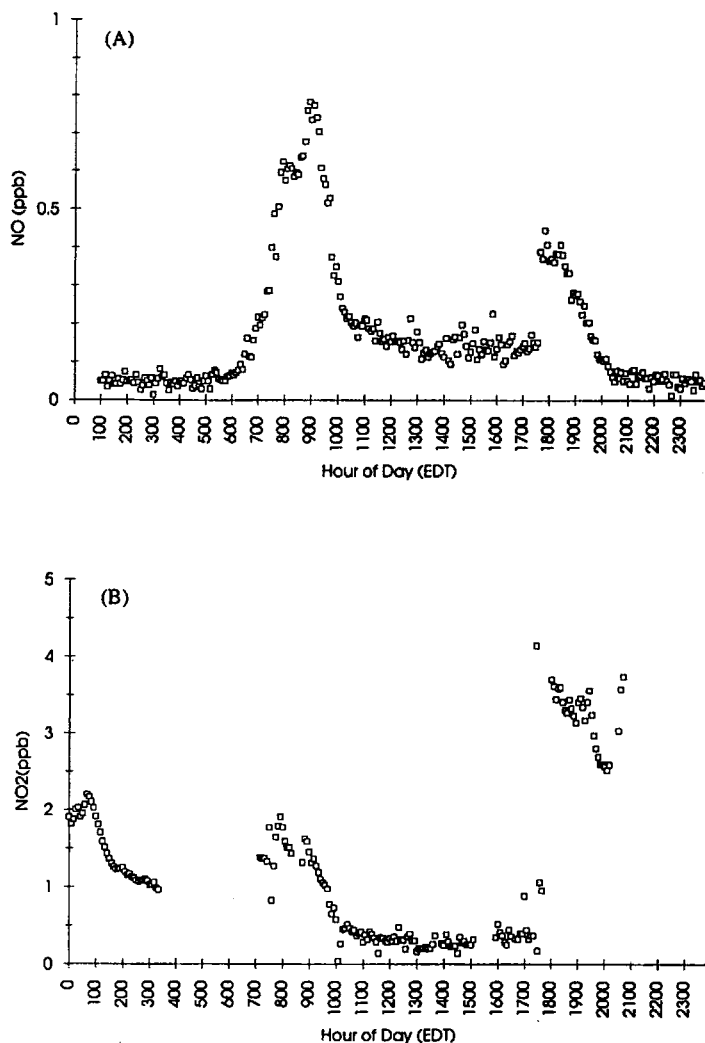


Fig. 2. Observed variation of (A) NO and (B) NO₂ at the Hastings site on 6 August 1992.

module, the chemistry of alkanes up to butane and the alkenes C₂H₄ and C₃H₆ are those proposed by Atkinson *et al.* (1982), and Atkinson and Lloyd (1984). In the present study, all anthropogenic alkanes with more than four carbon atoms were treated as *n*-butane while all anthropogenic alkenes with more than three carbon atoms were included in propene. Toluene is included to represent aromatic compounds while isoprene is used as the surrogate of natural hydrocarbons. The isoprene reaction scheme proposed by Lloyd *et al.* (1983) is used in the model. The reaction rate constants have been updated according

to the recommendations of JPL (1990) and IUPAC (1989).

In the vertical, the 1D photochemical transport model extends from 0 to the free troposphere. Vertical transport in the model is simulated by a diffusion process. The diffusion coefficients are derived through a micro-meteorological approach. The diurnal variations of the meteorological parameters and the diurnal variation of the planetary boundary layer (PBL) height are provided by a high-resolution planetary boundary layer model (Blakardar, 1979; Zhang and Anthes, 1982). Then, the values of the diffusion

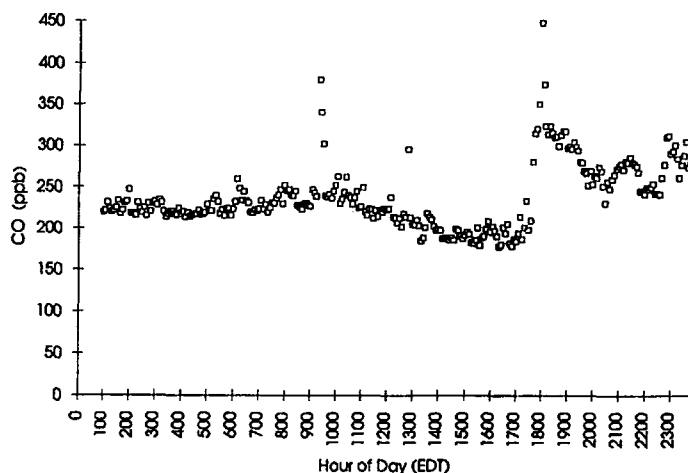


Fig. 3. Observed CO variation at the Hastings site on 6 August 1992.

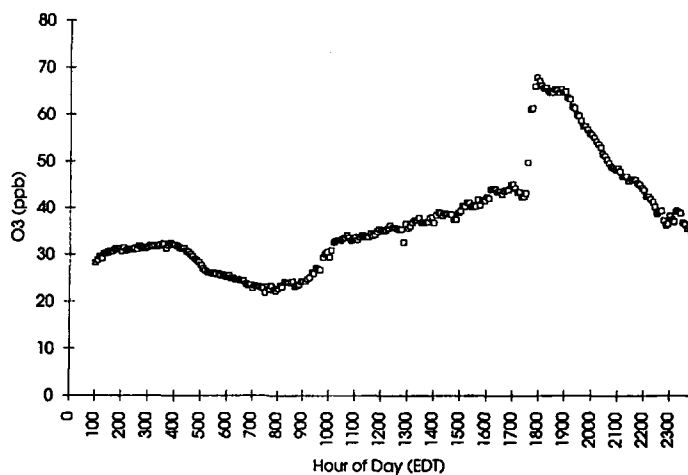


Fig. 4. Observed O₃ variation at the Hastings site on 6 August 1992.

coefficient are calculated for three different layers (0–80 m, 80 m–PBL height and above PBL height) (Trainer *et al.*, 1987). In the vertical diffusion calculation, the original advection calculation algorithm (Smolarkiewicz, 1983) was replaced with the implicit method of Richtmyer and Morton (1967). The latter was designed specifically for solving diffusion equations and ensure a fast and stable solution.

In addition, to account for the effect of mass exchange between the urban plume and the background air, a horizontal mixing algorithm was incorporated. As an urban plume travels, it experiences

mass exchange with its surrounding environment, i.e. the background. Phenomenologically, the mass exchange can be described by a dispersion process. In the present study the cross-wind length scale of the Greater Toronto urban plume, l (m), was assumed to increase linearly with time through

$$l = l_0 + \xi t \quad (1)$$

where l_0 is the initial value of l , t (s) is the lapse time after the plume is released, and ξ (m s^{-1}) is the rate of change of l . We set l_0 at 20,000 m. This value approximates the size of the Greater Toronto urban

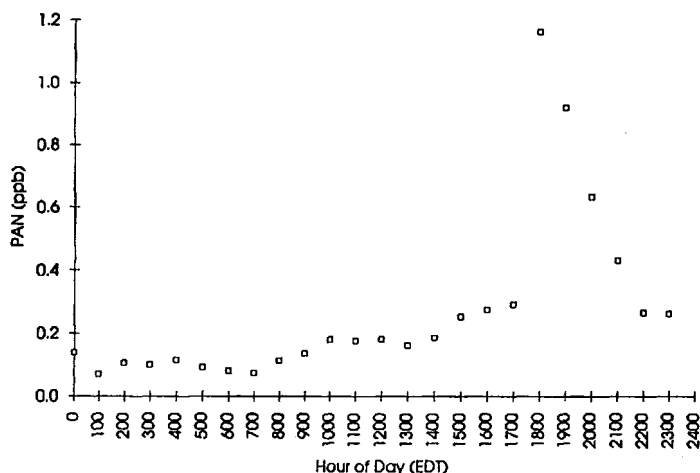


Fig. 5. Observed PAN variation at the Hastings site on 6 August 1992.

area. From the classical Gaussian dispersion theory, horizontal diffusivity k can be related to the horizontal dispersion parameter σ through

$$k \sim \sigma d\sigma/dt \quad (2)$$

assuming that diffusion is one order of magnitude smaller than advection in the atmosphere. Noticing the equivalence between σ and l , and using a scaling analysis, we may write

$$k \Delta C/l^2 \sim 0.1u \Delta C/l \quad (3)$$

where C stands for the concentration of a species being transported and u is the advective wind speed. We can solve (1)–(3) for l , ξ and k provided u is known. Based on the average surface wind speed measured at 10 m above ground at both the Binbrook and Hastings sites on 6 August 1992, we set u at 2.5 m s^{-1} . ξ is then estimated to be 0.25 m s^{-1} . This ξ gives a $5000 \text{ m}^2 \text{ s}^{-1}$ of horizontal diffusivity, k , for a 20-km wide puff. This value is within a reasonable range of the tropospheric diffusion data of Gifford (1982).

The model calculates temporal and vertical variations of chemical species along the trajectory, both inside and outside the plume. At each integration time step, the plume material undergoes horizontal mixing with the background. The concentration, C , of a species, after the mixing has taken place, is defined by

$$C = (C_p l + C_b \Delta l)/(l + \Delta l)$$

where Δl denotes the incremental change in the size of the urban plume during one time step, C_b is the concentration in the background air and C_p is the concentration within the plume.

3. DERIVATION OF INITIAL CONDITIONS

To simulate the observed impingement of the Greater Toronto urban plume at Hastings, we consider two adjacent air parcels, one representing the Greater Toronto urban plume and the other the background air. Both the air parcels evolve with time. At the impingement time, the difference between the simulated concentrations of various primary and secondary species in the two air parcels is expected to represent the concentration jumps observed at the Hastings site. To follow this approach, we first need to derive two sets of initial chemical systems for the two air parcels.

To derive the initial system for the air parcel representing the Greater Toronto urban plume, the 1D model was exercised in the Eulerian mode. In this Eulerian run, the Greater Toronto urban area was treated as a horizontal "box" with the dimensions of 20 and 30 km in the southeast–northwest and southwest–northeast axes, respectively. This area includes six municipalities, Etobicoke, Toronto, York, North York, East York and Scarborough. The 1985 southern Ontario emission inventory from the Ontario Ministry of Environment and Energy (OMEE) was used to derive averaged emission rates. Measured diurnal variations of O_3 , NO_x and various VOCs were used as the references for the model calculations to match. The emission rates were adjusted ($0.15 \text{ g m}^{-2} \text{ d}^{-1}$ for NO_x expressed as NO , $0.24 \text{ g m}^{-2} \text{ d}^{-1}$ for anthropogenic VOCs and $1.6 \times 10^{-3} \text{ g m}^{-2} \text{ d}^{-1}$ for isoprene) so that the diurnal variations of the species on the fifth model-day matched their measured counterparts. Through these exercises, we were able to derive a diurnally varying

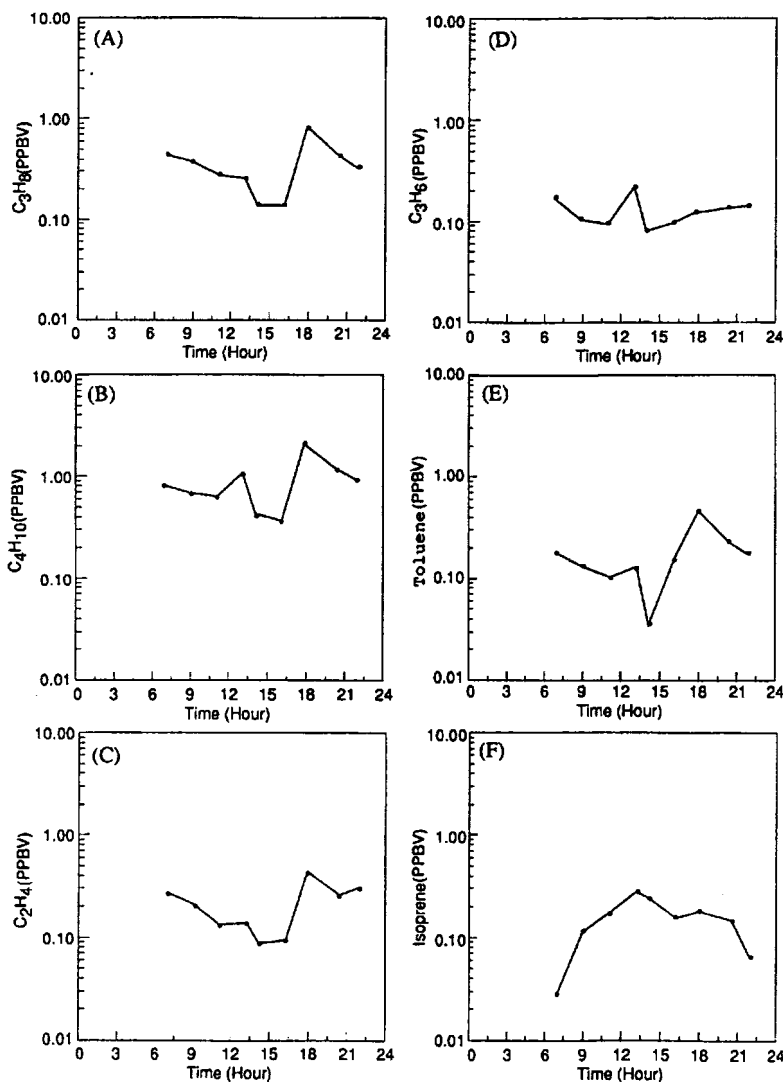


Fig. 6. Observed variations of (A) C_3H_8 , (B) C_4H_{10} , (C) C_2H_4 , (D) C_3H_6 , (E) toluene and (F) isoprene at the Hastings site on 6 August 1992.

system, which was chemically consistent, for the Greater Toronto urban plume.

For the air parcel associated with the Greater Toronto urban plume, the calculated diurnal variations of O_3 and NO_x were compared with the averaged ones derived from the measurements made at nine OMEE urban monitoring sites within the Greater Toronto urban area on 6 August 1992. The calculated diurnal variations of O_3 and NO_x are plotted in Fig. 7 and can be compared with their observed counterparts in Fig. 8. Evidently, the

calculated and the observed variations are in good agreement. It is worth noting that O_3 virtually vanishes at night in the urban area because of a fast titration by freshly emitted NO from the local traffic. It is seen that both the measured and observed diurnal variations of NO_x show two maxima. The first maximum is caused by the morning traffic before the break-up of the nocturnal inversion. The second maximum is attributed to the combined effect of the evening traffic and the formation of the near surface inversion. During the day, lower NO_x levels mainly

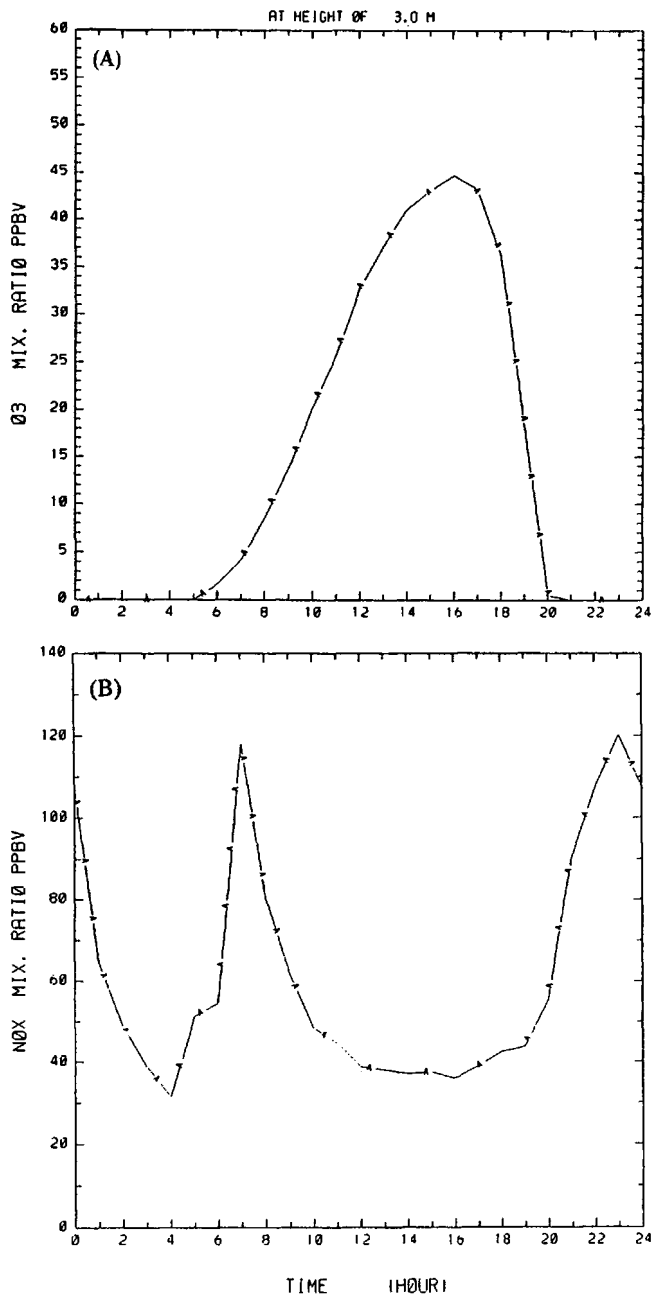


Fig. 7. Derived diurnal variations of (A) O₃ and (B) NO_x for the Greater Toronto urban area 6 August 1992. See text for details.

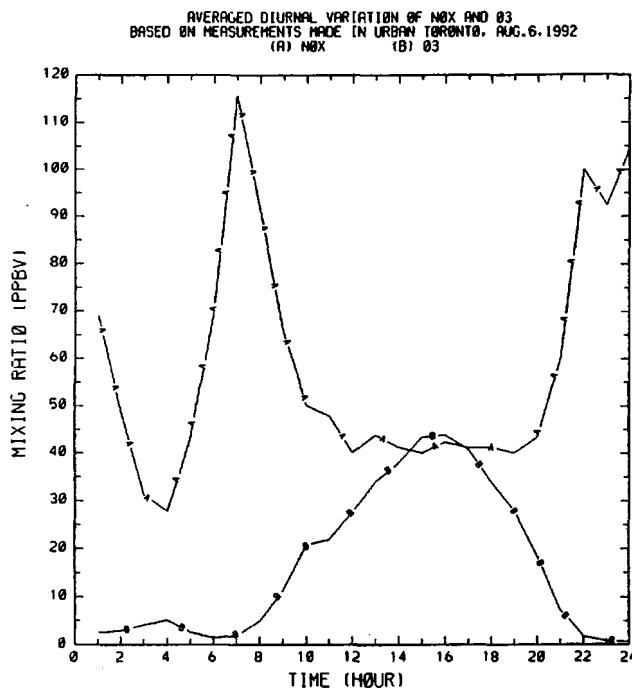


Fig. 8. Averaged diurnal variations of O₃ and NO_x observed at nine monitoring sites in the Greater Toronto urban area on 6 August 1992.

result from the dilution throughout a fully developed planetary boundary layer and the conversion to photooxidation products such as HNO₃, NO₃⁻, PAN, RONO₂, etc. Calculated diurnal variations of VOCs, presented in Fig. 9, were subjected to comparison with mid-afternoon measurements made at the York University campus, located in the Greater Toronto urban area, in July and August, 1991. Figure 10 gives the median levels and ranges of the VOC measurements made in the two summer months for the 180-degree northerly wind sector extending from west (270°) to east (90°). Apparently, the calculated mid-afternoon levels of various VOCs are comparable to these measurements.

A similar procedure was followed to derive the initial conditions for the background. The rural emissions were adjusted ($3.1 \times 10^{-3} \text{ g m}^{-2} \text{ d}^{-1}$ for NO_x expressed as NO, $2.6 \times 10^{-3} \text{ g m}^{-2} \text{ d}^{-1}$ for anthropogenic VOCs and $2.2 \times 10^{-3} \text{ g m}^{-2} \text{ d}^{-1}$ for isoprene) so that the calculated ground level concentrations fit the observed O₃, NO_x and VOC values. In this case, the measurement data obtained at both the Binbrook and Hastings sites on 6 August 1992 were used as the references. For the Hastings data, however, only those made before the impingement of the Greater Toronto urban plume were considered. The calculated initial

diurnal variations of O₃ and NO_x are presented in Fig. 11.

4. MODEL SIMULATIONS AND DISCUSSION

To simulate temporal variations of various chemical species at a fixed downwind distance in both the air parcels, we designed model runs as follows. Virtual receptors were set downwind of Toronto at 20 km intervals. Twenty-five consecutive puffs of the Greater Toronto urban plume were released at each hour. Model calculations of the Lagrangian type were then conducted for each of the 25 plume puffs. During the Lagrangian calculations, the rural emissions identical to the ones used in the derivation of the initial conditions for the background air were used. As the puffs passed over the receptors, the time of passage and the species concentrations both within the plume and in the background were registered. This procedure enabled us to construct complete diurnal variations of the species at various downwind distances for both the Toronto urban plume and the background. It should be noted that, in this study, the Lagrangian calculations were based on the surface wind as measured at 10 m above ground. Because of the existence of vertical wind shear, any model results for the free

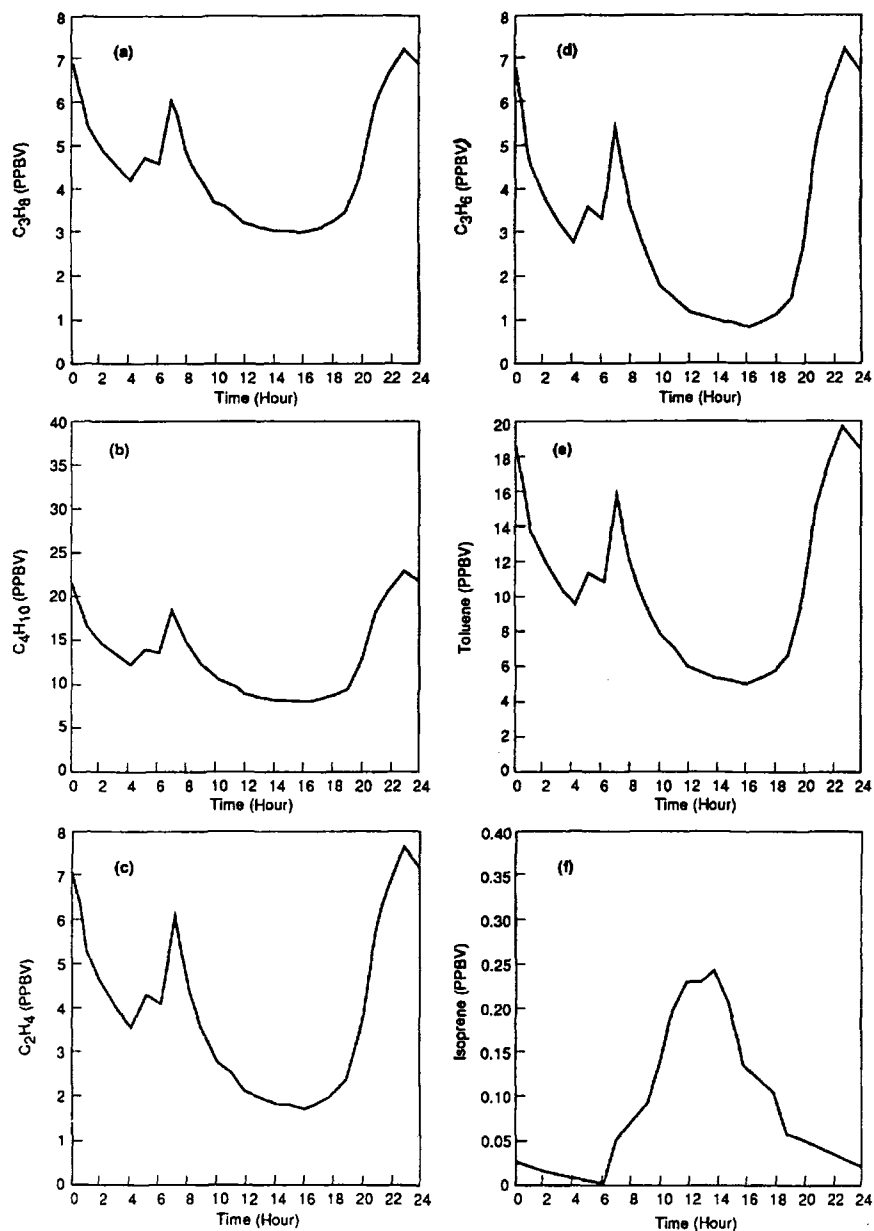


Fig. 9. Derived diurnal variations of (A) C_3H_8 , (B) C_4H_{10} , (C) C_2H_4 , (D) C_3H_6 , (E) toluene and (F) isoprene for the Greater Toronto urban area on 6 August 1992. See text for details.

troposphere over one day photochemical calculations would be meaningless. Thus, in the following, we will only concentrate on the values calculated for the level of 3 m above the ground.

Calculated diurnal variations of O_3 , PAN, NO, NO_2 , and VOCs at 140 km downwind for both the air parcels are plotted in Figs 12-15. The concentration differences between the two air parcels at 17:30 EDT,

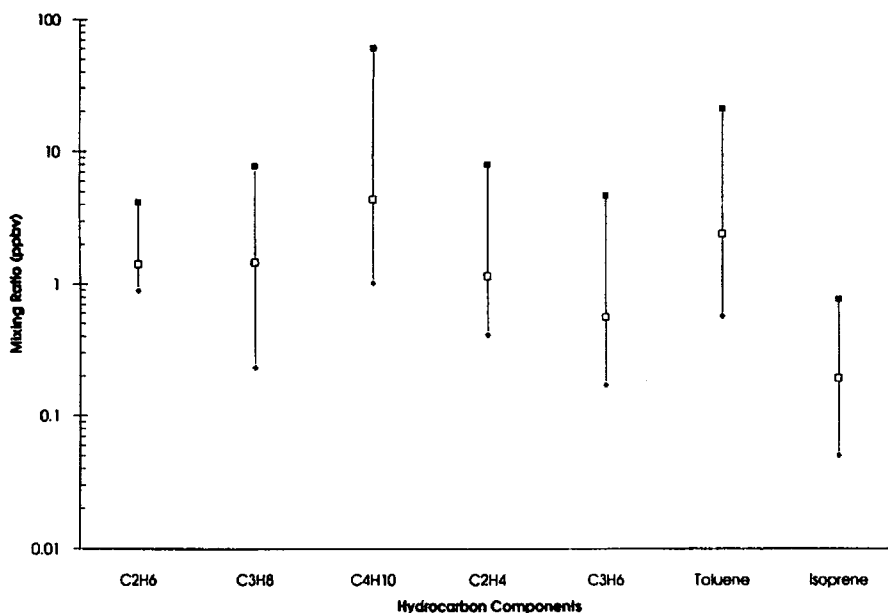


Fig. 10. Mid-afternoon levels of various VOCs sampled at the York University campus for the west-north-east wind sector in July and August, 1991. Blank squares denote the median values while vertical bars give the range of 90% data.

the impingement time, were compared with the observed increases in concentration at the Hastings site. It is seen that the calculated O_3 increase is 19 ppb which is comparable with the observed 25 ppb jump. For PAN, the model calculations reproduced the magnitude of the observed 1 ppb change from the clean background air to the polluted urban plume. As for NO_x and VOCs, the predicted changes are in reasonable agreement with the measurements. It is of interest to note that both calculations and observations show no significant changes for C_3H_6 and isoprene about the impingement time. This is consistent with the high reactive nature of the two hydrocarbon compounds.

To illustrate the impact of the Greater Toronto urban emissions on O_3 levels downwind further, we plotted daily maximum O_3 levels, in both the urban plume and the background, against downwind distance in Fig. 16. It is seen that, under the clean background conditions of 6 August 1992, the Greater Toronto urban emissions enhance O_3 production downwind and the enhancement increases with downwind distance.

According to the synoptic weather map of 6 August 1992, a high pressure centred in northwestern Pennsylvania and southern Ontario was under a weak west-southwesterly flow. Under this meteorological condition, wind field in the Toronto area are often influenced by lake-breeze flows. In the Lagrangian

modelling calculations, we treated the Greater Toronto urban plume in the cross-wind direction as a well mixed "box" with an initial cross-wind size of 20 km. Thus, we were not able to resolve any phenomenon associated with a smaller spatial scale, such as high O_3 levels in a narrow inland band paralleling the shore due to the lake-breeze induced fumigation under a light gradient wind condition (Lyons and Cole, 1976). In this study, the possible lake-breeze induced circulation was perpendicular to the synoptic wind direction and its horizontal scale (Roberts *et al.*, 1991) is comparable to the cross-wind size of the plume. The overall effect of the circulation on the urban plume "box" was parameterized by an enhancement of the horizontal (cross-wind) diffusivity. To account for this effect, we chose to increase the horizontal diffusivity in the following sensitivity tests.

Two sensitivity test runs were carried out to investigate the effect of the uncertainty in determining the horizontal (cross-wind) diffusivity. The first run used a diffusivity 10 times smaller than the one used in the above baseline run while the second run was conducted with a diffusivity 10 times larger than the baseline value. As discussed above, the second test represents an upper limit for the effect due to lake-breeze. Results from the two tests are presented in Fig. 17. It is seen that the results from the two runs confirm a general positive correlation between O_3 enhancement and downwind distance for the Toronto urban plume. The

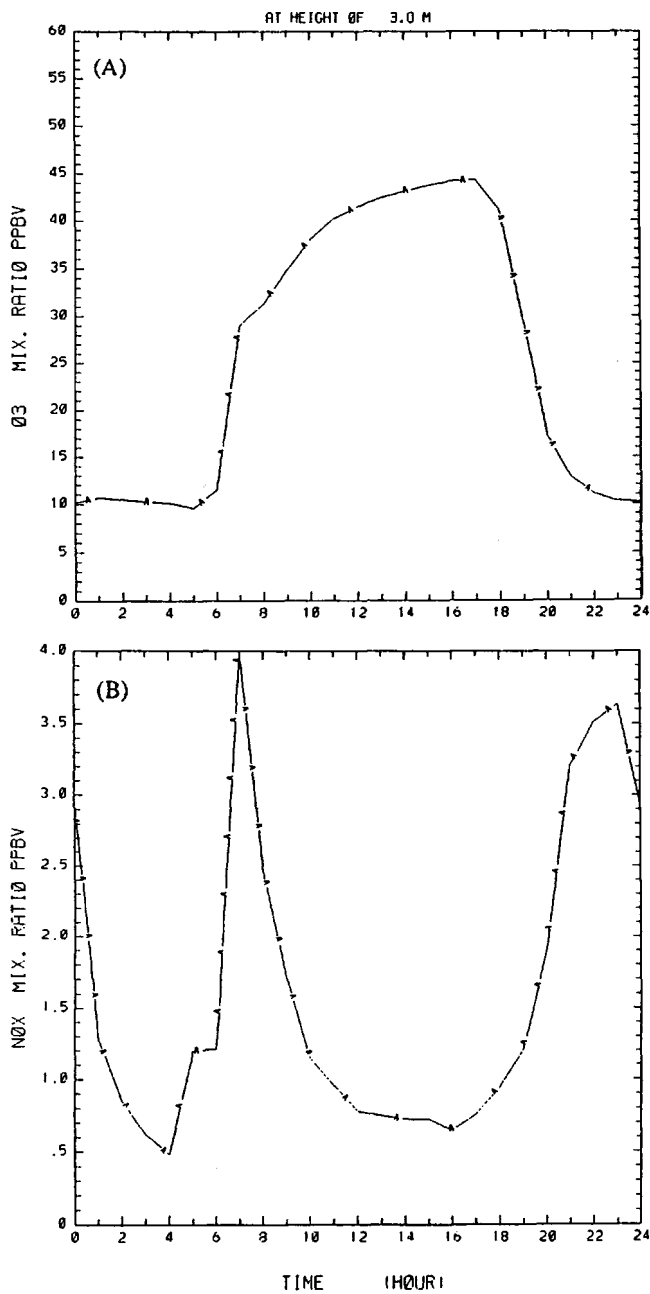


Fig. 11. Derived diurnal variations of (A) O₃ and (B) NO_x for the background on 6 August 1992. See text for details.

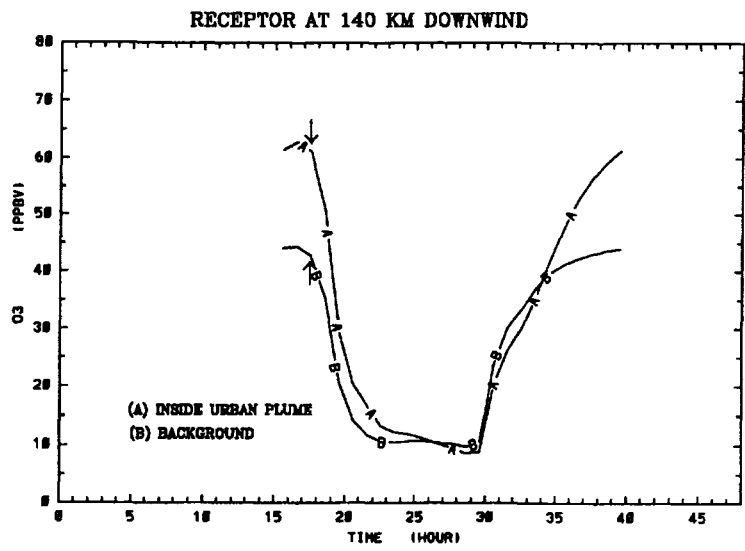


Fig. 12. Calculated variations of O₃ for both the Greater Toronto urban plume and background at 140 km downwind on 6 August 1992. The arrows indicate the impingement point.

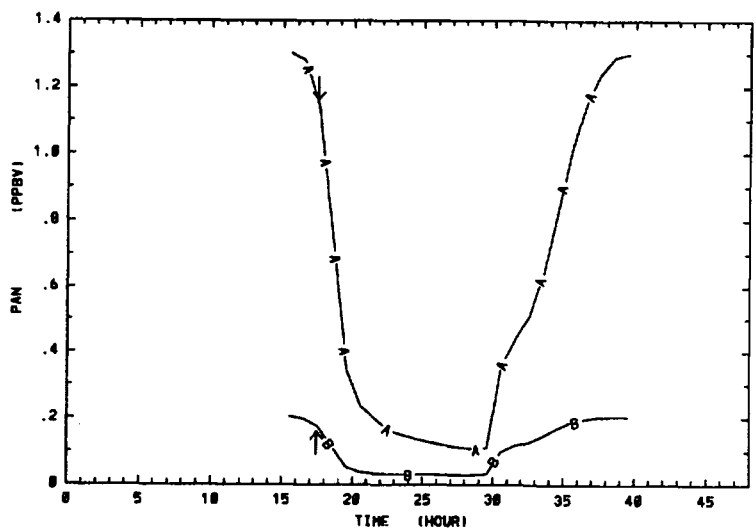


Fig. 13. Same as Fig. 11 but for PAN.

O₃ enhancement at 140 km downwind ranges from 7 to 24 ppb when the horizontal diffusivity varies over two orders of magnitude.

The effect of ambient temperature on the magnitude of the O₃ enhancement downwind of the Greater Toronto urban area was investigated. An increment

of 5°C was uniformly added to the observed diurnal temperature variations. Since the temperature-isoprene emission relation affects O₃ in both the urban plume and the background in a similar manner, we fixed the previously adjusted emissions in a test run to isolate the temperature effect only within the

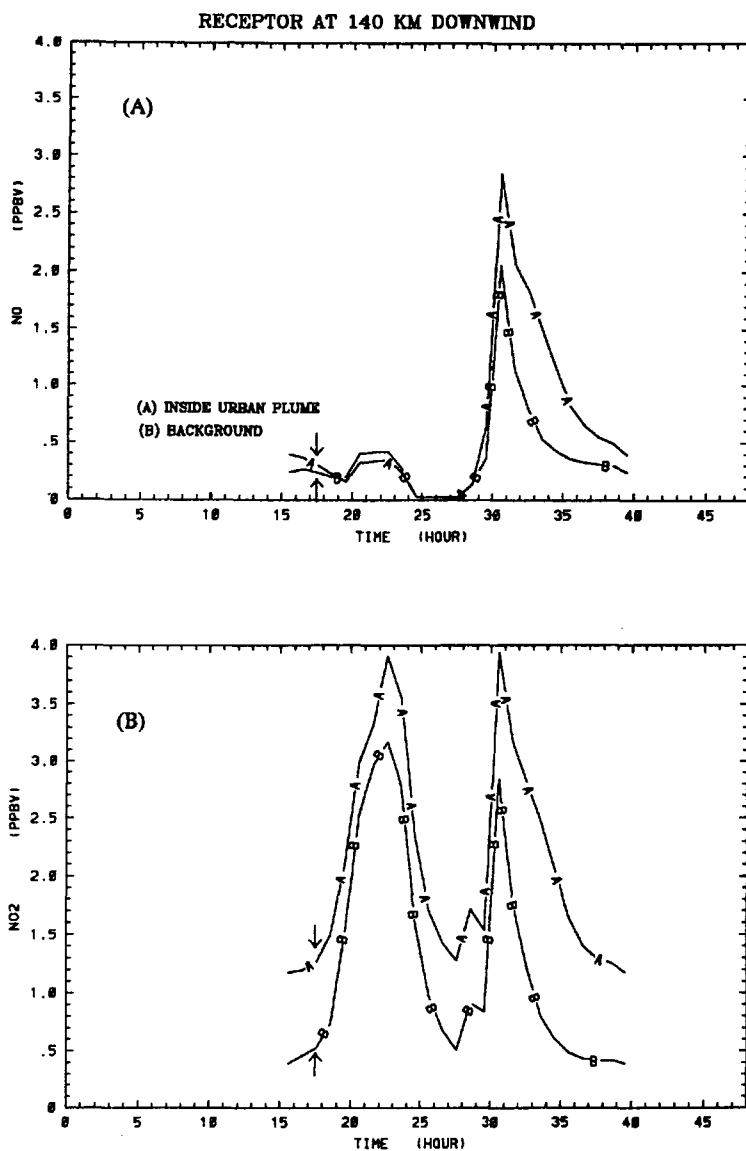


Fig. 14. Same as Fig. 11 but for (A) NO and (B) NO₂.

chemistry part. The test was started from the derivation of initial conditions. Then, the Lagrangian puff calculations were redone. In these calculations, all the parameters were kept identical to the ones used in the baseline runs except for the temperature. Calculated daily maximum O₃ levels in both the plume and background are plotted against downwind distance in Fig. 18.

The results, as compared with the ones in Fig. 16, suggest that, under the clean background condition an increase of temperature would lead to more O₃ production in the urban plume than in the background. Consequently, a larger O₃ enhancement due to the urban emissions would be expected for a warmer air mass. The temperature effect on the O₃ chemistry can be mainly attributed to the temper-

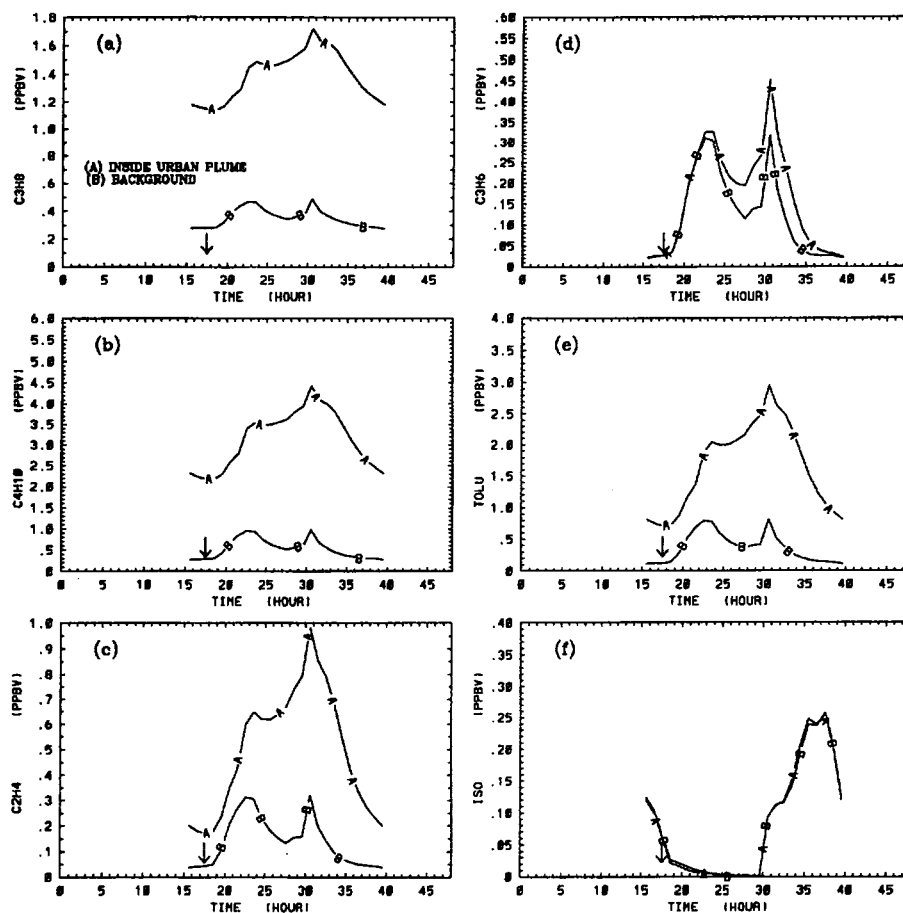


Fig. 15. Calculated variations of (A) C_3H_8 , (B) C_4H_{10} , (C) C_2H_4 , (D) C_3H_6 , (E) toluene and (F) isoprene for both the Greater Toronto urban plume and background at 140 km downwind on 6 August 1992. The arrows indicate the impingement point.

ature dependence of the PAN thermo-decomposition. The thermo-decomposition rate at noon on the modelled day would be increased from 2.74×10^{-4} to $5.85 \times 10^{-4} s^{-1}$ with a $5^\circ C$ temperature increase. In the urban plume, which has much higher PAN levels than the background (see in Fig. 13), this rate change would free more CH_3COO_2 radicals. As a result, more NO would be oxidized and more O_3 would be produced in the urban plume.

Finally, to check the effect of the photochemical reaction time on the O_3 enhancement downwind, we repeated the above baseline run but with an advective wind speed of $5 m s^{-1}$ which is twice the measured one. Results, as shown in Fig. 19, indicate that the difference in the daily O_3 maxima between the

Toronto urban plume and the clean background at 140 km downwind is reduced to 9 from 19 ppb in the baseline run. As the advective wind speed increases, the O_3 enhancement at a fixed distance is reduced.

5. CONCLUSION

In this study we used a 1D photochemical transport model to simulate the variations of primary and some important secondary photooxidant pollutants (NO_x , VOCs, O_3 and PAN) associated with an urban plume impingement, observed at the Hastings site on 6 August 1992. The calculated concentration jumps are in general agreement with the measurements. The results

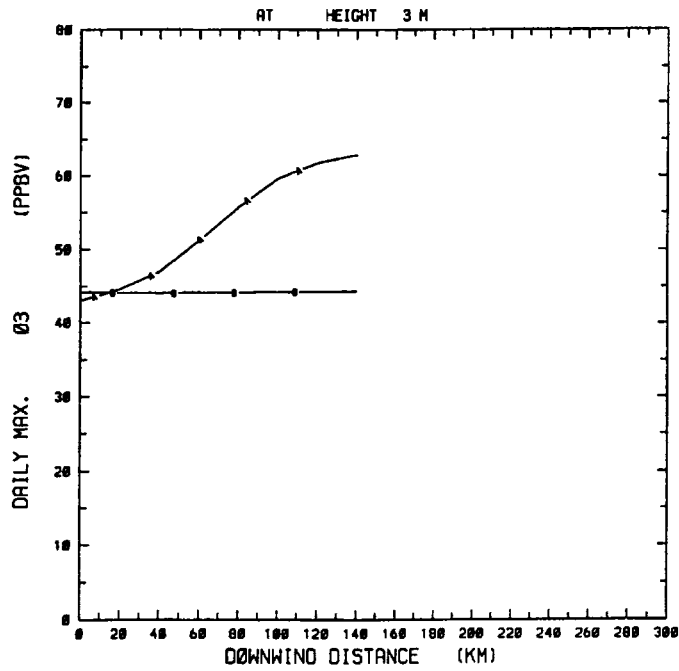


Fig. 16. Calculated variations of the daily maximum O₃ with the downwind distance under the conditions of 6 August 1992. Curve A gives the variations within the Toronto urban plume while curve B corresponds to the background.

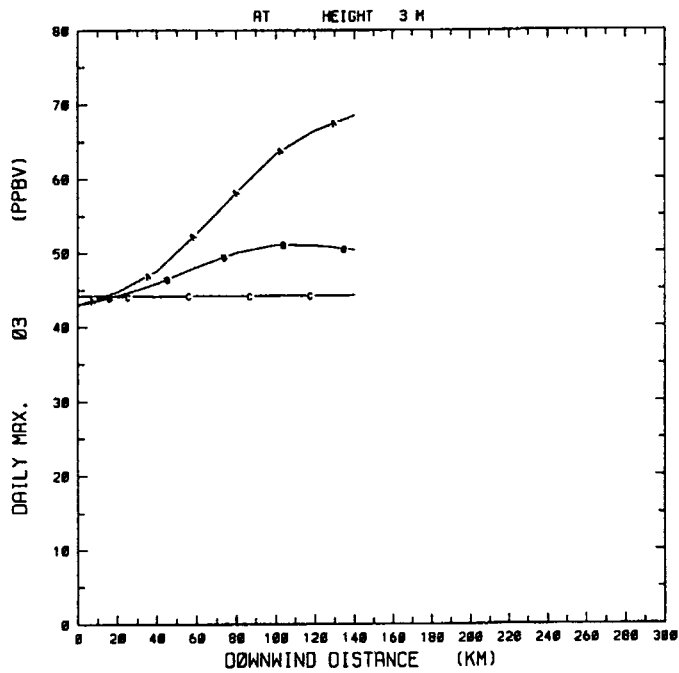


Fig. 17. Same as Fig. 16, but curve A corresponds to the urban plume with a slower horizontal dispersion ($\xi = 0.025 \text{ m s}^{-1}$); curve B corresponds to the urban plume with a faster horizontal dispersion ($\xi = 2.5 \text{ m s}^{-1}$); curve C corresponds to the background.

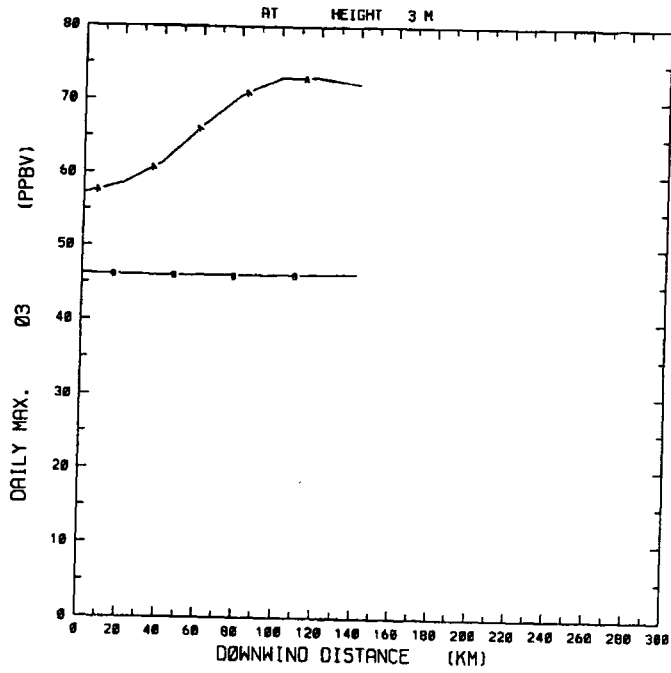


Fig. 18. Same as Fig. 16, but with the ambient temperature increased by 5°C. See text for details.

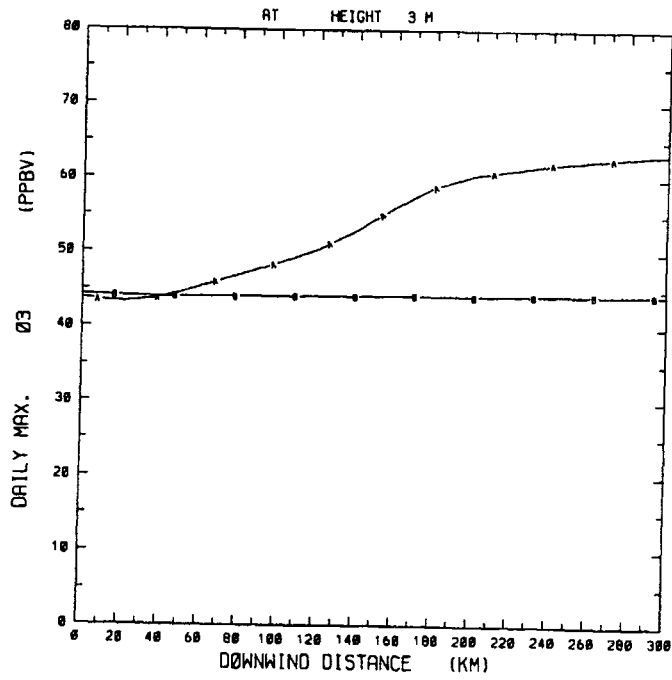


Fig. 19. Same as Fig. 16, but with the advective wind speed doubled to 5 m s⁻¹.

indicate that, under the clean background conditions of 6 August 1992, the Greater Toronto urban emissions enhanced O₃ production downwind and that the enhancement increased with downwind distance. Sensitivity tests on the horizontal diffusion rate further confirmed the positive correlation between O₃ enhancement in the urban plume and downwind distance. The O₃ enhancement at 140 km downwind ranges between 7 and 24 ppb when the horizontal diffusivity varies over two orders of magnitude.

A sensitivity test on the ambient temperature suggests that, under the clean background conditions, an increase of temperature would result in a larger O₃ enhancement in the Greater Toronto urban plume. A sensitivity test on the advective wind speed further shows a positive correlation between the O₃ levels downwind and the photochemical reaction time. Results of this study and more generalized investigation in the future will hopefully provide valuable information on the role of the Greater Toronto urban emission in O₃ production/destruction on a regional scale.

Acknowledgements—One of the authors, Xiude Lin, would like to thank Michael Trainer of the Aeronomy Laboratory, NOAA, for helpful discussions. SONTOS 92 is a Canadian Institute for Research in Atmospheric Chemistry research project, coordinated by Neville Reid, OMEE. This is a CIRAC (Canadian Institute for Research in Atmospheric Chemistry) contribution, # 95-2.

REFERENCES

- Atkinson R. and Lloyd A. C. (1984) Evaluation of kinetic and mechanistic data for modelling of photochemical smog. *J. phys. chem. Ref. Data* **13**, 315–444.
- Atkinson R., Lloyd A. C. and Wings L. (1982) An updated chemical mechanism for hydrocarbon/NO_x/SO₂ photooxidations suitable for inclusion in atmospheric simulation models. *Atmospheric Environment* **16**, 1341–1355.
- Angle R. P. and Sandhu H. S. (1989) Urban and rural ozone concentrations in Alberta. *Atmospheric Environment* **23**, 215–221.
- Blackadar A. K. (1979) High resolution models of the planetary boundary layer. In *Advances in Environmental Science and Engineering* (edited by Pfafflin J. and Ziegler E.), Vol. 1, pp. 50–85. Gordon and Breach, New York.
- Gifford F. A. (1982) Horizontal diffusion in the atmosphere: a Lagrangian-dynamical theory. *Atmospheric Environment* **16**, 505–512.
- Gladstone K. P., Niki H., Shepson P. B., Bottenheim J. W., Schiff H. I. and Sandhu H. S. (1991) Photochemical oxidant concentrations in two Canadian prairie cities: model evaluation. *Atmospheric Environment* **25B**, 243–254.
- IUPAC (1989) Evaluated photochemical data for atmospheric chemistry: supplement III. *J. phys. chem. Ref. Data* **89**, 881–1097.
- JPL (Jet Propulsion Laboratory) (1990) Chemical kinetics and photochemical data for use in stratospheric modeling. Evaluation Number 9. Calif. Inst. of Technol., Pasadena.
- Leahy D. M. and Hansen M. C. (1990) Observational evidence of ozone depletion by nitric oxide at 40 km downwind of a medium size city. *Atmospheric Environment* **24A**, 2533–2540.
- Lin X., Trainer M. and Liu S. C. (1988) On the nonlinearity of the tropospheric ozone production. *J. geophys. Res.* **93**, 15,879–15,888.
- Lin X., Melo O. T., Hastic D. R., Shepson P. B., Niki H. and Bottenheim J. W. (1992) A case study of ozone production in a rural area of central Ontario. *Atmospheric Environment* **26A**, 311–324.
- Liu S. C., Trainer M., Fehsenfeld F. C., Parrish D. D., Williams E. J., Fahey D. W., Hubler G. and Murphy P. C. (1987) Ozone production in the rural troposphere and the implications for regional and global ozone distribution. *J. geophys. Res.* **92**, 4191–4207.
- Lloyd A. C., Atkinson R., Lurman F. W. and Nitta B. (1983) Modelling potential ozone impacts from natural hydrocarbons—I. Development and testing of a chemical mechanism for the NO_x-air photooxidations of isoprene and α -pinene under ambient conditions. *Atmospheric Environment* **17**, 1931–1950.
- Lyons W. A. and Cole H. S. (1976) Photochemical oxidant transport: mesoscale lake breeze and synoptic-scale aspects. *J. appl. Met.* **15**, 733–743.
- Richtmyer R. D. and Morton K. W. (1967) *Difference Methods for Initial-Value Problems*, 2nd Edn, p. 405. Wiley, New York.
- Roberts P. T., Dye T. S., Hanna S. R. and Haga C. M. (1991) Data analysis for the Lake Michigan Ozone Study. Tropospheric ozone and the environment II: Effects, modelling, and control. In *Proc. Air and Waste Management Association Int. Speciality Conf.*, 4–7 November 1991, Atlanta, Georgia.
- Roussel P. B., Lin X., Camacho F., Laszlo S., Taylor R., Melo O. T., Shepson P. B., Hastic D. R. and Niki H. (1994) Observation of ozone and NO_x levels at two sites around Toronto, Ontario, during SONTOS 92. *Atmospheric Environment* (submitted).
- Sillman S., Samson P. J. and Masters J. M. (1993) Ozone production in urban plumes transported over water: photochemical model and case studies in the northeastern and midwestern United States. *J. geophys. Res.* **98**, 12,687–12,699.
- Smolarkiewicz P. K. (1983) A simple positive definite advection scheme with small implicit diffusion. *Mon. Weather Rev.* **111**, 479–486.
- Trainer M., Hsie E. Y., Mckeen S. A., Tallamraju R., Parrish D. D., Fehsenfeld F. C. and Liu S. C. (1987) Impact of natural hydrocarbons on hydroxyl and peroxy radicals at a remote site. *J. geophys. Res.* **92**, 11,879–11,894.
- Trainer M., Buhr M. P., Curran C. M., Fehsenfeld F. C., Hsie E. Y., Liu S. C., Norton R. B., Parrish D. D. and Williams E. J. (1991) Observations and modelling of reactive nitrogen photochemistry at a rural site. *J. geophys. Res.* **96**, 3045–3063.
- White W. H. and Patterson D. E. (1983) Urban export to the nonurban troposphere: results from project MISTT. *J. geophys. Res.* **88**, 10,745–10,752.
- Zhang, D. and Anthes R. A. (1982) A high-resolution model of the planetary boundary layer-sensitivity tests and comparisons with SESAME-79 data. *J. appl. Met.* **21**, 1594–1609.